J. At. Mol. Sci.
doi: 10.4208/jams.072513.101413a

Vol. **5** , No. 1, pp. 81-94
February 2014

Elastic properties and phonon dispersion of bcc vanadium under pressure from first principles

L. Q. Zhang[a,b], Y. Cheng[a,*], and Z. W. Niu[a]

[a] *Key Laboratory of High Energy Density Physics and Technology of Ministry of Education, Sichuan University, Chengdu 610064, China*
[b] *Department of Physics and Electronic Information, Huaibei Normal University, Huaibei 235000, China*

Received 25 July 2013; Accepted (in revised version) 14 October 2013
Published Online 18 November 2013

Abstract. We investigate the elastic properties and phonon dispersion of the body-centered cubic structure vanadium (V) under pressure by using the generalized gradient approximation (GGA). Our elastic constants of V at zero pressure and zero temperature are in good agreement with the available experimental data and other theoretical data. The pressure dependences of bulk modulus B and its pressure derivative B', shear modulus G, elastic Debye temperature Θ_E, elastic anisotropy factor A, Poisson ratios σ and Kleinmann parameter ζ are also presented. An analysis for the calculated elastic constants has been made to reveal the mechanical unstability of V up to 100 GPa. For the phonon dispersions of V, it is easily seen that the phonon frequencies increase as the volume decreases, the phonon mode linked to a Kohn anomaly has softened to negative values.

PACS: 71.15.Mb, 62.20.Dc, 77.84.Bw

Key words: vanadium; elastic properties; phonon dispersion; density functional theory

1 Introduction

Vanadium (V), one of the group-VB transition metals, crystallizes in the body-centered cubic (bcc) structure at ambient conditions. It has been attracted much more considerable attention due to its high thermal, low compressibility, and chemical stability. Up to date, many interesting on the fundamental physical and chemical properties of V have been reported in high-pressure experiments and theories [1-19].

Early in 1972, Simth [7] measured the superconducting transition temperature of V as a function of hydrostatic pressure up to 2.4 GPa and found a linear increase in T_c

*Corresponding author. *Email address:* ycheng66@qq.com (Y. Cheng)

with dT_C/dP=0.062 K/GPa. Later in 2000, Ishizuka *et al.* [8] reported a superconducting transition temperature of 17.5 K at 120 GPa. In addition, Skriver [9], Moriarty [10], and Grad *et al.* [11] predicted the stability of V in the bcc structure up to at least a couple of hundred GPa. Takemura [12] proved the speculation by diamond-anvil cell experiment. However, Ding *et al.* [13] measured a phase transition of V from the bcc structure to the rhombohedral phase at 69 GPa by the diamond-anvil cell and synchrotron X-ray diffraction method. Furthermore, Jenei *et al.* [14] identified a transition pressure at 30 GPa at room temperature through nonhydrostatic compression, which is much lower than the value reported by Ding *et al.* [13].

On the other hand, several theoretical methods have been applied to investigate the properties of V. Otani and his co-worker [5, 15] investigated the lattice dynamics of V in the pressure range up to 1.5 Mbar using full-potential linear muffin-tin orbital (FP-LMTO) method. They found that the transverse acoustic phonon mode shows a dramatic softening under pressure and becomes imaginary at pressure above 130 GPa, indicating the possibility of a structural phase transition. Lee *et al.* [16, 17] declared two different rhombohedral phases which differ from each other only in the angle between the rhombohedral basis vectors. Qiu and Marcus [18] obtained three first-order phase transitions from crossings of the Gibbs free energies functions curves. With the density functional perturbation theory (DFPT), Luo *et al.* [19] obtained the phase transitions [bcc→hR1(110.5°)→distorted hR2 (108.2°)→bcc] with the increasing pressure. Landa *et al.* [5] found that the structure transition from the bcc to rhombohedral phase at 60 GPa, and then to the bcc phase again at 310 GPa.

As is known that, the phonon-dispersion relations of the bcc structure V could not be determined by conventional inelastic neutron scattering techniques since its cross section for neutron scattering is almost totally incoherent [20]. Instead, people use the thermal diffuse scattering of X-rays to measure the phonon frequencies along principle symmetry directions [15, 21, 22]. The experimental phonon dispersion curve of bcc V at ambient conditions has been measured by thermal diffuse scattering and found that for the longitudinal (111) branch it exhibits a dip near the (2/3, 2/3, 2/3) site [20-22]. However, by using the inelastic X-ray scattering (IXS), Boska *et al.* [23] revealed several phonon-dispersion anomalies clearly, whereas few theoretical methods are applied to investigate the properties of phonon dispersion.

In this work, we focus on the elastic properties and phonon dispersion of V under pressure by the plane-wave pseudopotential density functional theory (DFT) method through the Cambridge Serial Total Energy package (CASTEP) program [24, 25]. The rest of the paper is organized as follows. The theoretical method and computation details are given in Section 2. Some results and discussion are presented in Section 3. Finally, the summary of our main results are given in Section 4.

2 Theoretical method and computation details

2.1 Total energy electronic structure calculations

In our electronic structure calculations, we employ two types of pseudopotentials, i.e. the norm-conserving (NC) and on-the-fly (OTF), for the interactions of the electrons with the ion cores, together with two types of functional forms for the exchange-correlation potential among electrons, i.e. the generalized gradient approximation (GGA) proposed by Perdew *et al.* [26] and the local density approximation (LDA) proposed by Vosko *et al.* [27]. The electronic wave functions are expanded in a plane wave basis set with an energy cut-off of 400 eV. The total energy and the ground state wave functions are calculated on a $10\times10\times10$ k-point mesh. Pseudo-atom calculation is performed for V $3d^3 4s^2$. The self-consistent convergence of total energy is 1.0×10^{-6} eV/atom. These parameters are carefully tested. It is found that these parameters are sufficient to lead to a well-converged total energy. All the total energy electronic structure calculations are implemented through the CASTEP code [24, 25].

The pressure-volume relationship can be obtained by fitting the calculated energy-volume $(E-V)$ data to the Vinet equation of state (EOS) [28]

$$\ln\left[\frac{Px^2}{3(1-x)}\right]=\ln B_0+\alpha(1-x),\quad x=\left(\frac{V}{V_0}\right)^{1/3} \tag{1}$$

where $V=V_0(0,T)$ is the zero-pressure equilibrium volume, derived by integration of the thermodynamic definition of the thermal expansion coefficient $\alpha(T)=V^{-1}\partial V/\partial T$,

$$V(0,T)=V(0,0)\exp\int_0^T\alpha(T)d(T) \tag{2}$$

$\ln B_0$ and $\alpha=3(B_0'-1)/2$ are the fitting parameters $B(P,T)$, $B'(P,T)$ are given by

$$B=-x^{-2}B_0e^{\alpha(1-x)}f(x) \tag{3}$$

$$B'=\left(\frac{\partial B_T}{\partial P}\right)_T=\frac{1}{3}\left[(\alpha x+2)-x\frac{f'(x)}{f(x)}\right] \tag{4}$$

where $f(x)=x-2-\alpha x(1-x)$.

2.2 Elastic properties

To investigate the elastic constants under pressure P, we use the symmetry dependent strains to be non-volume conserving. The elastic constants C_{ijkl} with respect to the finite strain variables is defined as [29-32]

$$C_{ijkl}=\left(\frac{\partial\sigma_{ij}(x)}{\partial e_{kl}}\right)_X \tag{5}$$

where σ_{ij} and e_{kl} are the applied stress and Eulerain strain tensors, and X and x are the coordinates before and after the deformation, respectively. For the isotropic stress, we have

$$C_{ijkl} = C_{ijkl} + P(2\delta_{ij}\delta_{kl} - \delta_{il}\delta_{jk}\delta_{ik}\delta_{jl})/2 \tag{6}$$

$$C_{ijkl} = \left(\frac{1}{V(x)}\frac{\partial^2 E(x)}{\partial e_{ij}\partial e_{kl}}\right)_X \tag{7}$$

where C_{ijkl} denotes the second-order derivatives with respect to the infinitesimal strain. The fourth-rank tensor C has generally 21 independent components. However, this number is greatly reduced when taking into account the symmetry of the cubic. For a bcc structure crystal, they are reduced to three, i.e. C_{11}, C_{44}, and C_{12}.

The adiabatic bulk B and the shear modulus G for a cubic crystal structure are taken as [33, 34]

$$B_V = B_R = (C_{11} + 2C_{12})/3 \tag{8}$$

$$G_V = (C_{11} - C_{12} + 3C_{44})/5 \tag{9}$$

$$G_R = 5(C_{11} - C_{12})C_{44}/[4C_{44} + 3(C_{11} - C_{12})]. \tag{10}$$

The arithmetic average of the Voigt and the Reuss bound is commonly used to estimate the polycrystalline modulus, in the term of the Voigt-Reuss-Hill approximations [33-35]

$$B = (B_V + B_R)/2 \tag{11}$$

$$G = (G_V + G_R)/2 \tag{12}$$

Then, Young's modulus E and Poisson's ratio σ can be calculated by

$$D = \frac{9BG}{3B+G}, \quad \sigma = \frac{1}{2}\left(1 - \frac{E}{3B}\right). \tag{13}$$

The elastic Debye temperature Θ_E may be estimated from the average sound velocity V_m [36]

$$\Theta_E = \frac{h}{k}\left[\frac{3n}{4\pi}\left(\frac{N_A\rho}{M}\right)\right]^{1/3} V_m, \tag{14}$$

where h is Planck's constants, k Boltzmann's constant, N_A Avogadro's number, n the number of atoms per formula unit, M the molecular mass per formula unit, ρ the density, and V_m is obtained from [36]

$$V_m = \left[\frac{1}{3}\left(\frac{2}{V_S^3} + \frac{1}{V_L^3}\right)\right]^{-1/3} \tag{15}$$

where V_S and V_L are the shear and longitudinal sound velocities, respectively. The values of the average shear and longitudinal sound velocities can be calculated from Navier's equations as follows [36]

$$V_S = \sqrt{\frac{G}{\rho}}, \quad V_L = \sqrt{\frac{(B+\frac{4}{3}G)}{\rho}}. \tag{16}$$

The Kleinmann parameter is an important parameter describing the relative position of the cation and anion sub-lattices. It is given by the following relation [37]

$$\zeta = \frac{C_{11}+8C_{12}}{7C_{11}+2C_{12}}. \tag{17}$$

By applying the method above, one has investigated successfully the elastic properties of several materials [38-43].

2.3 Phonon calculations

The harmonic approximation is usually a typical description for the physics of phonon, in which the equation of motion takes the form of [44]

$$\omega^2(k,l)e(k,l) = D(k)e(k,l), \tag{18}$$

where $\omega(k,l)$ is the phonon frequencies, $e(k,l)$ describing the corresponding atomic displacement, $D(k)$ is the dynamic matrix, which can be obtained from the force constant matrix Θ

$$D_{st}^{\alpha\beta}(k) = \frac{1}{\sqrt{M_t M_s}} \sum_R \Theta_{st}^{\alpha\beta}(R) \exp(-ik\cdot R), \tag{19}$$

where M_s and M_t are masses for atoms s and t, respectively, R is the Bravais lattice vectors. With the frame work of harmonic approximation, keeping only the second terms in the Taylor series of total energy E, Θ is given by

$$\Theta_{st}^{\alpha\beta} = \frac{\partial^2 E}{\partial \mu_s^\beta \partial \mu_t^\beta}, \tag{20}$$

where μ_s^α is the displacement for atom s from its equilibrium position in α direction. Consequently the force f exerted on atom s relating the displacement of atom t is

$$f = -\Theta_{st}\mu_t. \tag{21}$$

We perform the supercell method [45] to determine the dynamical matrix from Eq. (19), in which the forces are calculated with respect to the atoms perturbed from their equilibrium positions and frozen in.

Table 1: Equilibrium lattice parameter α, equilibrium volume V_0, the isothermal bulk modulus B_0, and its pressure derivation B_0' at $P=0$ and $T=0$, together with the experimental and other theoretical values.

	Methods	PSP	V_0 (Å^3)	α (Å^3)	B_0 (GPa)	B_0'
This work	GGA PAW	NC	13.936	3.03196	158.68	3.5895
		OTF	13.36	2.989686	192.02	4.1580
	LDA CA-PZ	NC	13.733	2.987579	182.11	3.2714
		OTF	12.5258	2.926035	228.45	3.8076
Cal.	GGA[46]		13.49	2.94	182	3.75
	GGA[5]			2.998	206	3.70
Exp.[13]			13.92	3.031	165	3.50

3 Results and discussion

3.1 Ground state structures of V

The EOS in the zero-tempera ture limit is the most fundamental characteristic describing the behavior of condensed matter at high pressures. Knowledge of the volume V variations with pressure P for a single phase determines the equilibrium volume V_0 and gives access to the bulk modulus B and the dimensionless pressure derivative of the bulk modulus B'. In our study, we take a series of different lattice constant α to calculate the total energy E corresponding to primitive unit cell volume V. The obtained lattice constant α, equilibrium unit cell volume V_0, bulk modulus B_0 and its pressure derivative B_0' with GGA and LDA calculations at 0 GPa and 0 K are also listed in Table 1, together with the available experimental and theoretical results for our comparison. It is shown that the equilibrium unit cell volume obtained from GGA-NC 13.936 Å^3 and GGA-OTF 13.36 Å^3 are less than the experimental value 13.92 Å^3 with the errors of 0.6% and 6.01%, respectively. The equilibrium unit cell volumes from LDA-NC and LDA-OTF are 13.333 Å^3 and 12.5258 Å^3, the corresponding errors are 5.3% and 7.56%, respectively. Thus, our results calculated from GGA-NC are more reliable when compared with the experimental data 13.92 Å^3 [13].

The lattice constant α from GGA method is slightly higher and that from LDA method is slightly lower (0.32% for GGA and 1.68% for LDA) than the experimental value (3.031 Å) [13]. The deviations of previous theoretical data of GGA [5, 46] are 3.33% and 1.08%, respectively. Thus, our results seem to be a little better. The isothermal bulk modulu B_0 of V is 158.68 GPa from GGA method and 182.11 GPa from LDA method, which are comparable to the values 206 GPa and 182 GPa calculated by other theoretical methods [5, 46], but more closely to the experimental values (165 GPa) [13]. On the other hand, the corresponding pressure derivative B_0' is 3.5895 from GGA calculation and 3.3214 from

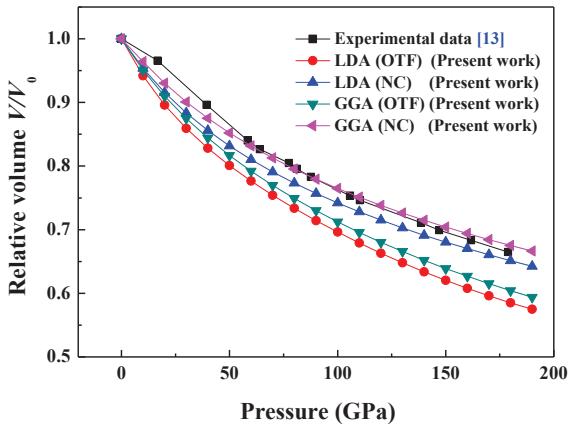

Figure 1: Relative volume V/V0 as function of pressure at 0 K from GGA (NC, OTF) and LDA (NC, OTF) methods.

LDA calculation are also in good agreement with the experimental result 3.50 with the error of 2.5% and 6.53%, respectively. From the above calculations, it is obvious that our GGA results are in better agreement with the experimental data [13] than our LDA results.

In Fig. 1, we illustrate the dependence of the calculated normalized volume V/V_0 (V0 is the zero pressure equilibrium primitive cell volume) of V on pressure P at 0 K. Our results from both LDA and GGA are slightly lower than the experimental data [13]. However, the results from GGA show good agreement with experimental data even slight discrepancies are still exist, as may be due to the fact that the experimental data are measured at room temperature, while our calculations are performed at zero temperature. On the other hand, each method has its own limitations related to the basic material parameters, basis sets, the precisions used, as well as the approximations of the method itself. Since the obtained lattice parameters from GGA-NC are the best, we apply it in the following calculations.

3.2 Elastic properties

Elastic properties of a solid are important because they are closely related to various fundamental solid-state phenomena, such as EOS, phonon spectra, and atomic potentials. To further confirm the structure stability under pressure, we calculate the elastic constants of the bcc V. The results are listed in Table 2, together with the available other calculated [46] and experimental [47] data. It is shown that the overestimation of C_{11} and C_{12} come from theoretical results of Koêi *et al.* [46] are closely to 14%, and C_{44} of Koêi *et al.* [46] is less than half of the reported experimental findings. However, our results show that C_{12} and C_{44} are more consistent with the experimental data of Alers *et al.* [47], while C_{11} is highly discrepant at 0 K. In contrast to C_{11} and C_{12}, the C_{44} was found to be relatively

Table 2: The elastic constant C_{11}, C_{44}, and C_{12} at P= 0 and T= 0, together with the experimental and other theoretical values.

	Methods	C_{11}	C_{44}	C_{12}
This work	GGA PAW (NC)	301.08	52.08	118.83
Cal.[46]	GGA (PAW)	260	17.1	135
Exp.[47]		232.4	45.95	119.36

Table 3: The elastic constants C_{11}, C_{44}, and C_{12} (GPa), aggregate elastic modulus B, B', shear modulus G, Young's modulus E, B/G, elastic Debye temperature Θ_E Kleinmann parameter ζ, Poisson ratio σ of the bcc V at 0 K and various pressure P (GPa).

P	C_{11}	C_{44}	C_{12}	B	G	B/G	σ	Θ_E	A	ζ
0	301.08	52.08	118.83	179.58	67.13	2.675	0.4975	541.29	5.90	0.533
10	352.45	51.67	155.21	202.95	150.26	0.444	0.4985	568.33	6.30	0.573
20	377.10	37.01	187.56	250.74	54.54	4.597	0.4981	619.09	6.67	0.622
30	393.60	12.82	222.67	279.65	30.66	9.121	0.4982	664.98	7.00	0.678
40	415.62	-20.54	254.85	308.44	-10.71	-28.79	0.4983	701.26	7.30	0.717
50	490.24	19.19	249.43	329.71	44.75	7.367	0.4985	729.27	7.58	0.62
60	563.68	40.85	263.80	363.76	71.05	5.119	0.4987	751.00	-0.850	0.59
70	630.99	54.88	287.75	402.16	88.49	4.544	0.4988	768.20	7.84	0.587
80	680.74	56.75	323.82	442.79	91.74	4.826	0.4989	782.26	8.08	0.604
90	701.09	33.87	354.62	470.11	93.78	0.640	0.4993	794.31	8.31	0.629
100	726.39	22.55	382.04	496.82	58.48	8.495	0.4990	805.31	8.73	0.646
150	834.84	-34.33	532.29	633.14	-13.75	-46.04	0.51	987.28	9.23	0.737
200	899.73	-207.09	606.21	710.71	-2935.94	-0.24	-4.93	1081.77	10.12	0.765
250	981.98	-174.08	747.67	825.78	-1554.7	-0.053	-1.28	1167.71	10.92	0.83
300	1421.55	10.94	816.58	1081.24	72.68	14.87	0.46	1256.18	11.66	0.68
350	1708.94	184.86	933.26	1191.82	248.92	4.76	0.40	1318.12	10.33	0.66

insensitive to pressure. The elastic constant C_{44} is greater than $(C_{11}-C_{12})/2$, which will lead to the degeneration of transverse branch in V, the situations are similar as the results of Ta [48]. At this stage, the elastic constant calculations as a function of pressure can only be used to detect the trends. Therefore, there is a need to investigate why the theoretical calculation of V shows such large discrepancies. To resolve this discrepancy, more theoretical computations are needed.

In Table 3, we list the elastic constant (C_{11}, C_{12}, and C_{44}) and elastic modulus B, pressure derivate B', shear modulus G, Poisson's ratios, B/G, elastic Debye temperature Θ_E, elastic anisotropy factor A, Poisson ratios σ, and Kleinmann parameter ζ for the bcc V under a wide range of pressures (0-350 GPa) at 0 K. It is seen that, the elastic constants C_{11}, C_{12}, bulk modulus B, increase monotonically with the applied pressure. However, when pressure increases up to 40 GPa, C_{44} becomes -20.54 GPa, and the shear modulus G becomes -10.71 GPa, indicating the mechanical instability of V, which is smaller than the experimental transition pressure 69 GPa [13]. However, Jenei *et al.* [14] reported the transition pressure 30 GPa at room temperature for nonhydrostatic compression, which

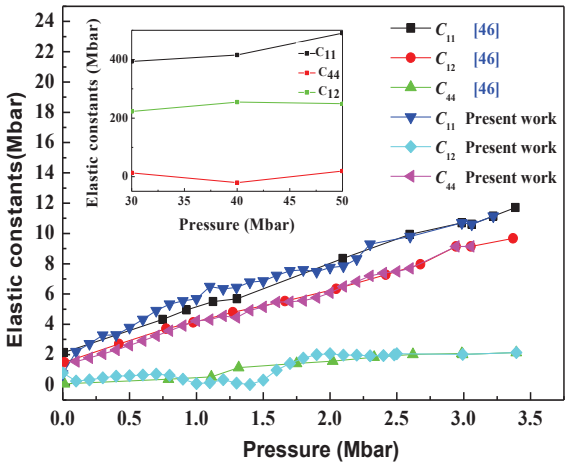

Figure 2: Elastic constants of the bcc structure V as a function of pressure (0-350 GPa), compared with those by Koêi *et al.* [46].

are more approximately with our results. An obvious difference in Fig. 1 is that the C_{11} and C_{12} show a steady, increasing behavior as a function of pressure, whereas the results from C_{44} are irregular. To clearly show the diversity, we plot the elastic constants of V under pressure (30-50 GPa) in Fig. 2, which shows that the elastic constants C_{11} and C_{12} increase monotonically with pressure, and are in excellent agreement with the theoretical data of Lee *et al.* [16], but the value of C_{44} decreases to negative when the applied pressure is larger than 40 GPa, and then gradually become positive again when the pressure increase to 50 GPa. A negative shear modulus means the material is mechanically unstable under monoclinic shear. The C_{44} diminishes to a negative value when the pressure is higher than 40 GPa, which is consistent with experiment [14].

It is acknowledged that the bulk modulus or shear modulus can measure the hardness in an indirect way [49]. Our results showed a very good match to the diamond-anvil cell data with $B = 185$ GPa and $G = 65$ GPa [50], but have a little discrepancy with the theoretical results of Luo *et al.* [19]. A high (low) B/G value is associated with ductility (brittleness). The critical value, which separates ductile and brittle materials, is about 1.75 [51]. Table 3 shows that the calculated values of B/G fluctuate with increasing of pressures, and the ductility and brittleness of V are unstable under higher pressure. Poisson's ratios, $\sigma = 0.25$ and 0.5, are the lower limit and upper limit in central force solids, respectively. In this work, Poisson's ratios increased with applied pressure. The obtained σ values are greater than 0.25, which indicates that the interatomic forces in the bcc V are central forces.

The Debye temperature is an important fundamental parameter and closely related to many physical properties of solids, such as the specific heat and melting temperature. From the elastic constants, one can obtain the elastic Debye temperature (Θ_E). The obtained elastic Debye temperatures of V under pressure are also presented in Table 3.

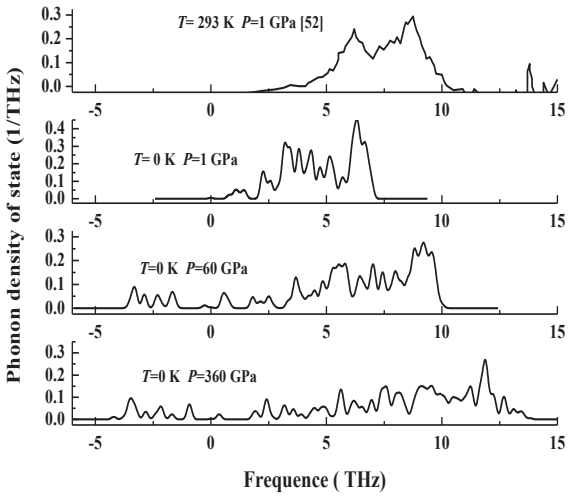

Figure 3: Calculated PDOS of the bcc structure V at pressures 1 GPa, 60 GPa and 360 GPa, compared with those by Bogdanoff *et al.* [52].

For V at 0 K and 0 GPa, we yield $(\Theta_E) = 541.29$ K from the elastic constants of GGA-NC calculations, however, which is considerably higher than the values 399.3 K determined from velocity-of-sound measurement [47]. Our elastic constants B are excellent with those of Alers *et al.* [47] and Bosak *et al.* [23], which fit the elastic moduli from the long-wavelength dispersions.

3.3 Phonon dispersions

Fig. 3 shows the phonon density of states (PDOS) of the bcc structure vanadium as a function of pressure. It is easily seen that the phonon frequencies increase as the volume decreases. The lower frequency phonon mode is found to be grown and softened, and other phonon frequencies move to higher values with the increasing pressure. At $P = 60$ GPa, the negative frequency appears in the PDOS, however which still keeps the character of the bcc structural spectrum, whereas with the increase of pressure, the PDOS shows a different profile of the frequency distribution, meaning the dynamic instability of the bcc vanadium. Bogdanoff *et al.* [52] confirmed that the PDOS had little changed up to 1273 K, and a large softening at 1673 K. In Fig. 3, we compare our calculated 0 K phonon density of state at 1 GPa, 60 GPa, and 360 GPa with the experiment observed by Bogdanoff *et al.* [52]. The behavior of the PDOS leads us to conclude that volume compression and rising temperature exert equal role. With the enhanced pressure or compressive volume, the phonon scattering are remarkable.

Using the supercell method, we have performed the GGA calculations for the 0 K phonon dispersions of V up to 400 GPa. We measured all the phonon branches along high symmetry direction in Fig. 4. Our results are in remarkable agreement with the

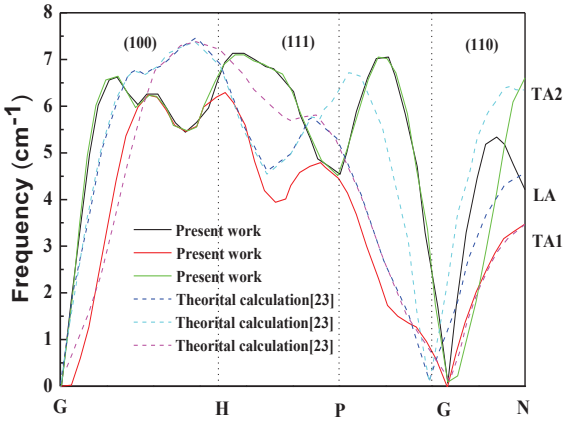

Figure 4: Calculated phonon dispersions of the bcc structure V at ambient pressure compared with those by Bosak *et al.* [23].

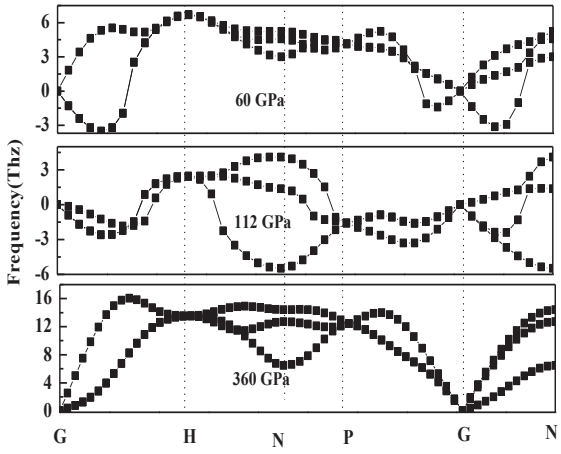

Figure 5: Calculated phonon dispersion of the bcc structure V at 60 GPa, 112 GPa and 360 GPa.

phonon dispersions derived from IXS by Bosak *et al.* [23]. The phonon band structure of V and its behavior under pressure are shown in Fig. 5, where the calculations for the phonon dispersion curves are along the high symmetry direction G-H-P-G-N for the bcc structure V at zero temperatures, where the high symmetry k-points H, P and N are (1/2, -1/2, 1/2), (1/4, 1/4, 1/4) and (0, 0, 1/2), respectively. Obviously, there are two branches, one is the LA mode and the other degenerated TA1 and TA2 modes along the [110] direction. There exists a crossover between the LA mode and the TA2 mode at zone boundary point N. The transverse dispersion curve for TA2 is higher than those of the longitudinal dispersion curve near the [110] symmetry direction.

To further research the properties of the phonon dispersions of V under pressures, we chose three pressures 60 GPa, 112 GPa, and 360 GPa, respectively. From Fig. 5, when the

pressure is up to 60 GPa, the phonon spectra near G point is imaginary frequency. The imaginary frequencies in the phonon dispersion indicate mechanical instabilities, which can lead to phase transformations. Using synchrotron X-ray diffraction, Ding *et al.* [13] declared a phase transition at 63-69 GPa at room temperature. The imaginary frequencies at 60 GPa agrees reasonably well with the experimental data. When the pressure is up to 112 GPa, it is still unstable (the imaginary frequencies of the soft modes are still there). There appears a deep dip of the LA mode in N direction, showing that the bcc structure V is unstable under the pressure. When $P = 360$ GPa, the imaginary frequencies disappears, but the Kohn anomaly is still there. Luo *et al.* [19] investigate the lattice dynamics of V under high pressure with density functional perturbation theory (DFPT). Their calculations show that the lattice dynamical instability starts at 62 GPa, which results in the phase transition from bcc to hR1 (alpha=110.5°). While at pressure around 130 GPa, the rhombohedral angle of hR1 phase changed to 108.2°. When the pressure increases to 250 GPa, the bcc structure is stable again. These results are consistent with our results.

4 Summary

The bcc structure V has been investigated with the norm-conserving pseudopotential scheme in the frame of the generalized gradient approximation (GGA). Based on the GGA calculations, we have obtained the lattice parameters, isothermal bulk modulus and its pressure derivative of V at zero pressure and zero temperature. The results obtained agree well with the available experimental data and other theoretical results. With the increase of the applied pressure, the C_{44} becomes softening, as had been proved by the available experimental data and other theoretical data. The pressure dependence of the elastic constants, elastic modulus, Kleinmann parameter ζ, elastic Debye temperature, Poisson's ratio, and mechanical anisotropy of V has also investigated. It is found that the bcc structure V demonstrates brittleness when the pressure is higher than 10 GPa, and presents ductility under higher pressure. Moreover, we have performed the GGA calculations for phonon dispersions of V. It is easily seen that the phonon frequencies increase as the volume decreases, the phonon mode linked to a Kohn anomaly has softened to negative values, which can induce a high symmetry loss.

Acknowledgments The authors would like to thank the support for the computational resources by the State Key Laboratory of Polymer Materials Engineering of China in Sichuan University.

References

[1] V. V. Struzhkin, Y. A. Timofeev, R. J. Hemely, and H. K. Mao, Phys. Rev. Lett. 79 (1997) 4262.
[2] J. S. Tse, Z. Li, K. Uehara, Y. Ma, and R. Ahuja, Phys. Rev. B 69 (2004) 132101.
[3] H. Cynn and C. S. Yoo, Phys. Rev. B 59 (1999) 8526.
[4] N. Suzuki and M. Otani, J. Phys.: Condens. Matter 14 (2002) 10869.

[5] A. Landa, J. Klepeis, P. Souderlind, I. Naumov, O. Velikokhatnyi, L. Viots, and A. Ruban, J. Phys.: Condens. Matter 18 (2006) 5079.
[6] A. Dewaele, P. Loubeyre, and M. Mezouar, Phys. Rev. B 70 (2004) 094112.
[7] T. F. Smith, J. Phys. F: Met. Phys. 2 (1972) 246.
[8] M. Ishizuka, M. Iketani, and S. Endo, Phys. Rev. B 61 (2000) 3823.
[9] H. L. Skriver, Phys. Rev. B 31 (1985) 1909.
[10] J. A. Moriarty, Phys. Rev. B 45 (1992) 2004.
[11] G. B. Grad, P. Blaha, J. Luitz, K. Schwarz, A. Fernandez Guillermet, and S. J. Sferco, Phys. Rev. B 62 (2000) 12743.
[12] K. Takemura, J. Appl. Phys. 89 (2001) 662.
[13] Y. Ding, R. Ahuja, J. Shu, P. Chow, W. Luo, and H. K. Mao, Phys. Rev. Lett. 98 (2007) 085502.
[14] Z. Jenei, H. P. Liermann, H. Cynn, J. H. P. Klepeis, B. J. Baer, and W. J. Evans, Phys. Lett. B 83 (2011) 054101.
[15] S. Otani, J. Crystal Growth. 192 (1998) 346.
[16] B. Lee, R. E. Rudd, J. E. Klepeis, P. Söderlind, and A. Landa, Phys. Rev. B 75 (2007) 180101(R).
[17] B. Lee, R. E. Rudd, J. E. Klepeis, and R. Becker, Phys. Rev. B 77 (2008) 134105.
[18] S. L. Qiu and P. M. Marcus, J. Phys.: Condens. Matter 20 (2008) 275218.
[19] W. Luo, R. Ahuja, Y. Ding, and H. K. Mao, PNAS 104 (2007) 42.
[20] JR. Colella and B.W. Batterma, Phys. Pev. B 1 (1970) 3913.
[21] K. Matsubayashi, M. Maki, T. Moriwaka, T. Tsuzuki, T. Nishioka, C. H. Lee, A. Yamamoto, T. Ohta, and N. K. Sato, J. Phys. Soc. Jpn. 72 (2003) 2097.
[22] S. Otani and T. Mori, J. Mater. Sci. Lett. 22 (2003) 1065.
[23] A. Bosak, M. Hoesch, K. Antonangeli, D. L. Farber, I. Fischer, and M. Krisch, Phys. Rev. B 78 (2008) 023031R.
[24] M. C. Payne, M. P. Teter, D. C. Allen, T. A. Arias, and J. D. Joannopoulos, Rev. Mod. Phys. 64 (1992) 1045.
[25] V. Milman, B. Winker, J. A. White, C. J. Packard, M. C. Payne, E. V. Akhmatskaya, and R. H. Nobes, Int. J. Quantum. Chem. 77 (2000) 895.
[26] J. P. Perdew, K. Burke, and M. Ernzerhof, Phys. Rev. Lett. 77 (1996) 3865.
[27] S. H. Vosko, L. Wilk, and M. Nusair, Can. J. Phys. 58 (1980) 1200.
[28] P. Vinet, J. H. Rose, J. Ferrante, and J. R. Smith, J. Phys.: Condens. Matter 1 (1989) 1941.
[29] J. H. Wang, J. Li, S. Yip, S. Phillpot, and D. Wolf, Phys. Rev. B 52 (1995) 12627.
[30] D. C. Wallace, Thermodynamics of Crystals (Wiley, New York, 1972).
[31] B. B. Karki, G. J. Ackland, and J. Crain, J. Phys.: Condens. Matter 9 (1997) 8579.
[32] T. H. K. Barron and M. L. Klein, Proc. Phys. Soc. 85 (1965) 523.
[33] D. W. Voigt, Lehrbuch der Kristallphysik (Taubner, Leipzig, 1928).
[34] A. Reuss, Z. Angew. Math. Mech. 9 (1929) 49.
[35] R. Hill, Proc. Soc. London A 65 (1952) 349.
[36] O. L. Anderson, J. Phys. Chem. Solids 24 (1963) 909.
[37] W. A. Harrison, Elastic Structure and Properties of Solids (Freeman, San Francisco, 1980).
[38] X. F. Li, G. F. Ji, F. Zhao, X. R. Chen, and D. Alfe, J. Phys.: Condens. Matt. 21 (2009) 025505.
[39] J. Chang, X. R. Chen, Y. Cheng, and J. Zhu, Physica B 405 (2010) 529.
[40] J. Chang, X. R. Chen, W. Zhang, and J. Zhu, Chin. Phys. B 17 (2008) 1377; X. L. Zhou, K. Liu, X. R. Chen, and J. Zhu, Chin. Phys. B 15 (2006) 3014.
[41] H. H. Chen, Y. Bi, Y. Cheng, G. F. Ji, and L. C. Cai, J. Phys. Chem. Solids 73 (2012) 1197.
[42] X. L. Yuan, D. Q. Wei, Y. Cheng, Q. M. Zhang, and Z. Z. Gong, J. At. Mol. Sci. 3 (2012) 177.
[43] P. Wang, Y. Cheng, X. H. Zhu, X. R. Chen, and G. F. Ji, J. Alloy. Comp. 526 (2012) 74.

[44] E. Kaxiras, Atomic and Electronic Structure of Solids (Cambridge University Press, New York, 2003).
[45] S. Baroni, S. de Gironcoli, A. Dal Corso, and P. Giannozzi, Rev. Mod. Phys. 73 (2001) 515; A. van de Walle and G. Ceder, Rev. Mod. Phys. 74 (2002) 11.
[46] L. Koêi, Y. Ma, A. R. Oganov, P. Souvatzis, and R. Ahuja, Phys. Rev. B 77 (2008) 214101.
[47] G. A. Alers, Phys. Rev. 119 (1960) 1532.
[48] A. D. B. Woods, Phys. Rev. 136 (1964) A781.
[49] D. M. Teter, MRS Bull. 23 (1960) 1531.
[50] A. K. Verma and P. Modak, High Pressure Physics Division, Bhabha Atomic Research Centre (Trombay, Mumbai, India).
[51] S. F. Pugh, Phil. Mag. 45 (1954) 833.
[52] P. D. Bogdanoff, B. Fultz, J. L. Robertson, and L. Crow, Phys. Rev. B 65 (2002) 014303.